

AD-A107 920

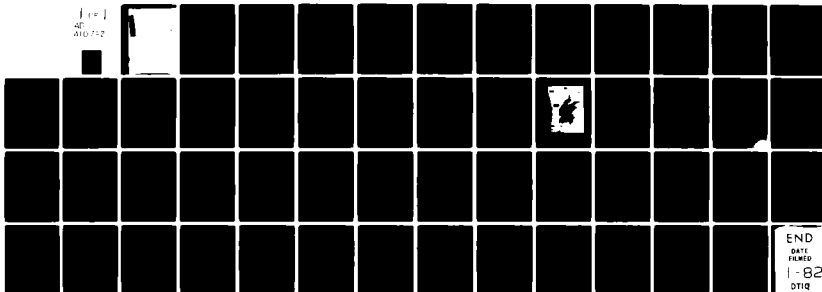
NAVAL RESEARCH LAB WASHINGTON DC
FCT SIMULATION OF HOB AIRBLAST PHENOMENA, (U)
SEP 81 A L KUHL, M A FRY, M PICONE, D L BOOK
NRL-MR-4613

F/6 18/3

UNCLASSIFIED

NL

1 of 1
40
010/112



END
DATE
FILMED
1-82
DTIC

AD A107920

(12) 54

SECURITY CLASSIFICATION OF THIS PAGE (When Data Entered)

REPORT DOCUMENTATION PAGE		READ INSTRUCTIONS BEFORE COMPLETING FORM
1. REPORT NUMBER NRL Memorandum Report 4613	2. GOVT ACCESSION NO. AD A107920	3. RECIPIENT'S CATALOG NUMBER
4. TITLE (and Subtitle) FCT SIMULATION OF HOB AIRBLAST PHENOMENA		5. TYPE OF REPORT & PERIOD COVERED Interim report on a continuing NRL problem.
		6. PERFORMING ORG. REPORT NUMBER
7. AUTHOR(s) A. L. Kuhl*, M. A. Fry**, M. Picone, D. L. Book and J. P. Boris		8. CONTRACT OR GRANT NUMBER(s)
9. PERFORMING ORGANIZATION NAME AND ADDRESS Naval Research Laboratory Washington, DC 20375		10. PROGRAM ELEMENT PROJECT, TASK AREA & WORK UNIT NUMBERS 62715H; 44-0578-0-1
11. CONTROLLING OFFICE NAME AND ADDRESS Defense Nuclear Agency Washington, DC 20305		12. REPORT DATE September 29, 1981
		13. NUMBER OF PAGES 53
14. MONITORING AGENCY NAME & ADDRESS (if different from Controlling Office)		15. SECURITY CLASS. (of this report) UNCLASSIFIED
		15a. DECLASSIFICATION/DOWNGRADING SCHEDULE
16. DISTRIBUTION STATEMENT (of this Report) Approved for public release; distribution unlimited.		
17. DISTRIBUTION STATEMENT (of the abstract entered in Block 20, if different from Report)		
18. SUPPLEMENTARY NOTES *Present address: R & D Associates, P.O. Box 9695, Marina del Rey, California 90291 **Present address: Science Applications, Inc., McLean, Virginia 22102 (Continues)		
19. KEY WORDS (Continue on reverse side if necessary and identify by block number) HOB (Height-of-burst) Hemispherical HE (High explosive) Airblast Environment Detonation(s) Overpressure		
20. ABSTRACT (Continue on reverse side if necessary and identify by block number) Height-of-burst (HOB) detonations can create airblast environments which are more severe than surface burst environments at high overpressures (>100 psi). A double Mach stem structure develops during shock reflection from the ground at a range approximately equal to the HOB. This creates double peak static pressure waveforms with enhanced early-time impulses. Blast diffraction on above ground structures also (Continues)		

DD FORM 1 JAN 73 1473

EDITION OF 1 NOV 65 IS OBSOLETE
S/N 0102-014-6601

SECURITY CLASSIFICATION OF THIS PAGE (When Data Entered)

file

18. Supplementary Notes (Continued)

This work was supported by the Defense Nuclear Agency under Subtask XY99QAXSG, work unit 00001, and work unit title "Flux-Corrected Transport."

This paper was presented at the Seventh International Symposium on Military Applications of Blast Simulation, July 13-17, 1981, Medicine Hat, Alberta, Canada, under the title "Simulation of High Overpressure HOB Airblast Environments on a Large Scale."

20. Abstract (Continued)

contains multiple peaks with enhanced loads and impulses. There is an ongoing interest in simulating these HOB environments for military applications. High explosives (HE) charges can be used to simulate the nuclear surface burst case below about 100 psi for reasonable yields (100T or more), but it appears that it is impractical to elevate large HE charges above grade to simulate the HOB case. In this paper we propose a new method for naturally simulating such HOB environments on a large scale. A hemispherical HE charge could be detonated near a natural slope which had been graded to form a large ramp. When the spherical blast wave reflects from this ramp a shock structure and environment is created which is similar to the HOB case. Validity of this concept is demonstrated by numerical simulations with a nonsteady 2-D FCT hydrocode. These calculations indicate that a 30° ramp located 200 ft from a 500T hemispherical HE charge will create 400 to 600 psi double peak static pressure waveforms at distances of 40 to 60 ft up the ramp; time between peaks is 1 ms. These waveforms correspond to a nuclear detonation at 100 to 120 ft/ $KT^{1/3}$ and a ground range of 190 to 210 ft/ $KT^{1/3}$.

↑

to the
1/3 power

CONTENTS

I. INTRODUCTION	1
II. CONCEPTUAL DESIGN OF THE HOB SIMULATOR	3
III. COMPUTATIONAL TECHNIQUE	4
IV. CALCULATIONAL RESULTS	6
V. SUMMARY AND CONCLUSIONS	8
VI. RECOMMENDATIONS	9
ACKNOWLEDGMENTS	9
REFERENCES	23

Accession For	
NTIS GRA&I	<input checked="" type="checkbox"/>
DTIC TAB	<input type="checkbox"/>
Unannounced	<input type="checkbox"/>
Justification	
By _____	
Distribution/	
Availability Codes	
Dist	Avail and/or Special
A	

DTIC
ELECTED
DEC 1 1981
D

FCT SIMULATION OF HOB AIRBLAST PHENOMENA

I. INTRODUCTION

It is now recognized that height-of-burst (HOB) detonations can create more severe airblast environments than surface burst (SB) detonations, especially at high overpressures. In the HOB case, the spherical blast wave reflects from the ground, initially as a regular reflection. Then at a ground range approximately equal to the height-of-burst, the shock reflection makes a transition to a double Mach shock structure. This double shock structure creates secondary peaks in the static pressure at and near the ground and thus enhances the early-time HOB airblast impulses compared to the SB case. As shown experimentally by H. J. Carpenter at MABS-IV (Ref. 1), these secondary peaks of the HOB case can be much greater than the first peaks.

When a double Mach shock structure reflects from an above-ground structure, it can produce enhanced diffraction loads. HOB diffraction loads are compared with SB loads in Fig. 1 which was constructed by scaling data from the 1000-lb Pentolite sphere experiments on the recent MIGHTY MACH test series (Ref. 2). As is evident from this figure, the early-time HOB loading impulses are about twice the SB values. Similar effects are shown in Fig. 1 for the static pressure histories and impulses which apply to loads on flush mounted structures.

For military applications, there is a need to simulate these HOB blast environments on a large scale in order to test the response and survivability of large-scale or full-scale military systems. Explosive yields from kilotons to megatons are required. Suspension of such large high explosive (HE) charges is impractical and could lead to poor quality blast fields due to interference effects from the charge support structure.

In this paper we propose a novel approach for simulating HOB blast environments on a large scale. The concept is shown in Fig. 2. A hemispherical surface burst HE charge would be used to create a free-field blast wave. The charge would be situated near an up-slope which had been graded to form a large ramp. When the spherical blast reflects from the ramp, a double Mach shock structure can be created (within certain constraints on wedge angle, θ_w , and incident shock Mach number). This concept relies on the similarity between the HOB-produced environments on horizontal surfaces and the environments produced by shock reflections on wedges or ramps. In Fig. 3 we compare some recent

Manuscript submitted July 22, 1981.

calculations with the FAST2D code:* a nuclear detonation at $HOB = 10^4 \text{ ft/KT}_N^{1/3}$ versus a Mach seven square wave shock reflection from a wedge. The pressure contours show that for similar shock strengths and angles, the shock structures in the wedge and HOB cases are qualitatively similar; density contours are also qualitatively similar with a slip line emanating from the primary triple point. There are, however, quantitative differences: the Mach stem structure in the nuclear HOB case is more complex, with a bulge at the foot of the Mach stem; also, in the nuclear case, the reflected shock races rapidly through the high temperature (10^4 to 10^5 °K) fireball, while in the wedge case, the reflected wave propagates slowly into the lower ($\sim 10^3$ °K) temperature constant field behind the incident square wave shock. We believe, however, that these differences are of secondary importance.

A remaining question is: how well does the blast wave from a hemispherical HE charge simulate the nuclear free-field environment? In Figure 4 we compare the static and dynamic pressure waveforms for the HE and nuclear cases from Brode's one-dimensional (1-D) free air burst calculations (Refs. 3,4) at shock overpressures of approximately 100, 200 and 400 psig. In the HE case a contact surface (CS) separates the air from the detonation products. This contact surface causes a sharp jump in dynamic pressure due to the high densities of the products. Also evident in the HE case is a secondary shock, S_2 , which faces inward but is being swept outward by the rapid expansion of the charge. The HE-driven blast wave gives a rather poor simulation of the complete nuclear waveform at high overpressures, due principally to the HE contact surface and secondary shock. However, the HE blast wave outside the contact surface is a reasonably good simulation of the nuclear case. We propose to use precisely this part of the HE blast wave and reflect it from the ramp to simulate the early-time nuclear HOB cases.

The remainder of the paper is organized as follows: Section II gives a conceptual design of the ramp HOB simulator; Section III describes the 2-D finite difference scheme which we used to investigate numerically the flow fields on and near the ramp; Section IV presents the results of these calculations, while conclusions and recommendations are offered in Sections V and VI.

* This code uses the Flux Corrected Transport (FCT) algorithm, described in Section III, to maintain sharp discontinuities.

II. CONCEPTUAL DESIGN OF THE HOB SIMULATOR

The design objective for this simulator is to produce the high overpressure (say 100 to 1000 psi) double-peak flow fields which simulate nuclear HOB detonations in the Mach reflection regime with high fidelity. The simulator should be reasonably inexpensive and readily constructed. The design concept should be extendable to large yields.

The primary design parameters for the simulator are the location of the front edge of the ramp, GR_R , and the ramp angle, θ_W . The conceptual design process begins with an HE free-air pressure-range curve for 1 lb of Pentolite. A ramp was assumed to be located at a GR_R corresponding to free field shock overpressures of 500 psi or 150 psi. Assuming various ramp angles, we used reflection factors (Ref. 1) to determine the peak static pressure versus ramp ground range, RGR . Parametric results are presented in Fig. 5. Inserts give the results scaled to a 500T surface burst which are equivalent to about a one-kiloton nuclear surface burst case. Examination of the results in Fig. 5 indicates the following trends:

- o A requirement for a high pressure (400 psi to 600 psi) simulator forces one to either move the ramp closer to the charge, or increase the ramp angle, or both.
- o One would prefer to move the ramp away from the charge so that the HE free field is close to the nuclear case; however, this leads to large (and presumably impractical) ramp angles.
- o Decreasing the ramp angle tends to make the Mach stem rise more rapidly thus increasing the separation between the first and second peaks; we speculate that this could lead to a yield amplification on the front-end of the waveform.
- o Transition to Mach reflection occurs at the leading edge of the ramp for $\theta_W = 30^\circ$ and 40° ; the transition point (TP) for the $\theta_W = 60^\circ$ occurs at about one-half the distance up the ramp.

The 30° ramp at the 500 psi station appears to be an interesting case--it is feasible to construct and the 600-psi shock overpressure will occur at about 50 ft up the ramp, thus allowing plenty of time for the Mach stem height to grow. Peak pressures will range from 1500 psi at the beginning of the ramp to about 300 psi at the far end.

III. COMPUTATIONAL TECHNIQUE

A numerical simulation of the shock diffraction for the ramp HOB simulator (a 30° ramp starting at 200 feet from a 500T hemispherical HE charge) was performed with a nonsteady two-dimensional (2-D) hydrocode, FAST2D. The objectives of the calculation were to validate the ramp HOB simulator design and to evaluate, in detail, the flow field in the vicinity of the ramp. The FAST2D code solves the balance laws of gasdynamics on a sliding grid in the general form:

$$\frac{\partial}{\partial t} \int_{\delta V(t)} \phi dV = - \oint_{\delta A(t)} \phi (\underline{u} - \underline{u}_g) \cdot d\underline{A} + \oint_{\delta A(t)} \tau dA \quad (1)$$

where ϕ represents the mass, momentum, energy or species mass density (for multi-material calculations) in cell $\delta V(t)$, \underline{u} and \underline{u}_g represent the fluid and grid velocities, respectively, and τ represents the pressure/work terms. The finite-difference approximation to Eq. (1) uses a vectorized Flux-Corrected Transport (FCT) algorithm, ETBFCT (Ref. 5), which gives an accurate and well-resolved description of shock wave propagation without the necessity of an a priori knowledge of the number, location or character of the gasdynamic discontinuities in the problem. The linear portion of this algorithm is fourth-order-accurate spatially for constant-velocity advection problems, and has a nonlinear flux-corrected antidiffusion stage which automatically provides the local dissipation needed to accurately model discontinuities. The formulation of the algorithm allows the grid to slide with respect to the fluid without introducing additional numerical diffusion. This general adaptive regridding technique permits fine zones to be concentrated in the region of greatest physical interest, thus reducing computational costs with no serious loss in resolution.

Since the ETBFCT algorithm is one-dimensional, time-splitting must be employed to solve two-dimensional problems. Time-splitting makes the boundary condition on the ramp particularly easy to implement. The ramp is represented as a series of "stairsteps" (of varying height and depth) along the interface between the extremal interior zones and a corresponding set of guard cells. A guard cell is defined as the right-most cell in the r -direction during the r -sweep, and the bottom-most cell in the z -direction during the z -sweep. The stairstep boundary conditions are reflective, which requires pressure, density and energy to be continuous and the corresponding velocity normal to the stairstep to vanish.

The numerical simulation began with a 1-D FCT calculation of the blast wave driven by a one pound spherical charge of PBX-9404 in air. The initial conditions, which are shown in Fig. 6, were taken to be the self-similar flow field corresponding to a spherical Chapman-Jouguet detonation wave (Ref. 6), at the time the detonation wave reaches the charge radius, $r_0 = 3.89 \text{ cm/lb}^{1/3}$. A Jones-Wilkins-Lee (JWL) equation of state (EOS) was used for the detonation products and a real air equation of state was used outside the HE/air interface. These EOS specify the pressure as a function of density and internal energy. The HE/air interface was followed by solving a conservation law for the mass fraction ϕ (where $\phi=1$ in the pure HE and $\phi=0$ in the pure air). The equations of state were blended in the mixed cells ($0 < \phi < 1$) according to Dalton's law. A fixed grid of 500 cells was used with a mesh spacing $\Delta r = 0.1025 \text{ cm/lb}^{1/3}$, so that the initial flow field in the charge occupied about 38 computational cells. The flow field results at the end of the 1-D calculation (cycle 1281, $t = 152 \text{ } \mu\text{s/lb}^{1/3}$) are shown in Fig. 6. The shock overpressure is 445 psig. The density distribution shows a jump at the HE/air interface; inside the interface is a secondary inward-facing shock which is being swept outward by the supersonic flow.

These results were scaled up to the 500 ton HE surface burst case by multiplying all times and ranges by the scale factor, $SF = (2 \times 10^6)^{1/3} = 125.992$. The shock radius at this time of $19.15 \text{ ms}/500T^{1/3}$ was found to be $198 \text{ ft}/500T^{1/3}$ with an overpressure of 445 psig (note that this point checks with the HE free air curve in Fig. 5). These results were then inserted as initial conditions in the cylindrical r - z FAST2D code, with one approximation. Since the γ 's ahead and behind the HE/air interface were quite close ($\gamma_{HE} = 1.25$ versus $\gamma_{air} = 1.30$), the HE products were modeled with the real air equation of state, and the 2-D interface was not followed specifically with a mass species conservation law. The 2-D mesh consisted of 150×150 cells with a moving fine mesh region (55×55 cells, $\Delta r = 5 \text{ cm}$ and $\Delta z = 2.8868 \text{ cm}$ with $\Delta z/\Delta r = \tan 30^\circ$) which followed the Mach stem. The calculation was run 5601 cycles. Diagnostics for the 2-D calculation consisted of 46 environment time histories (at 40 stations on the ramp and 6 stations perpendicular to the ramp at a RGR = 60.5 ft) and contour plots of the flow field every 200 cycles. Times are denoted by the label $\Delta t = t - t_0$, which references everything to the incident shock arrival time at the foot of the ramp $t_0 = 19.2 \text{ ms}$.

IV. CALCULATIONAL RESULTS

An overall picture of the spherical shock reflection from the ramp is displayed in Fig. 7 which gives the calculated pressure and density contours at various times ($\Delta t = 3, 5.61, 9.27$ and $13.4 \text{ ms}/500T^{1/3}$); Fig. 8 gives a magnified view of the flow field at $\Delta t = 9.61 \text{ ms}/500T^{1/3}$. The shape of the shock structure for the simulator (i.e., the geometry of the incident wave, the Mach stem, and the kinked reflected wave) more closely resemble the shock structure for square wave reflections from a ramp (Ref. 7) than the nuclear HOB case (see Fig. 3). The density contours indicate that a contact surface (a slip line) emanates from the triple point (the confluence of the incident, Mach and reflected waves) and approaches the ramp at an angle of about 60° . Pressure contours indicate that a high pressure region is located in the vicinity of where the projection of the contact surface would strike the ramp.

Figure 9 gives an experimental shadowgraph of the shock wave structure formed by an 8 lb TNT driven blast wave ($\text{HOB} = 1.04 \text{ ft}/\text{lb}^{1/3}$) diffracting on a 31° ramp. The incident shock pressure was about 120 psi at the foot of the ramp and about 75 psi at the time of the photograph (compliments of W. Dudziak, Ref. 8). The shock structure is qualitatively similar to that in Figs. 7 and 8. Fig. 9 shows that the reflected wave pushes the TNT products away from the ramp, thus maintaining a clean air flow (unpolluted by HE products) in the Mach stem region--a truly beneficial result! Note that this happens even in the low HOB case where the TNT products squish along the ground and push the TNT/air interface closer to the shock.

The calculated shock properties for the ramp HOB simulator are shown in Fig. 10 as a function of ramp ground range, RGR. The primary Mach stem pressure, p_1 , ranged from about 600 psi to 400 psi. The second peak pressure, p_2 , decayed from 1300 psi at the foot of the ramp to 400 psi at the 60 foot station. The peak pressures were determined from two methods: for $\text{RGR} < 30 \text{ ft}$ peaks were evaluated from pressure distributions at a fixed time, and these data are somewhat noisy due to the staircase boundary condition modeling of the ramp; for $\text{RGR} > 30 \text{ ft}$, peaks were evaluated by smoothing the pressure time histories two cells above the ramp, giving a smooth pressure-range curve.* Note that the second peaks are in reasonably good agreement with

* Unfortunately the pressure histories for $\text{RGR} < 30 \text{ ft}$ were not available for data analysis.

the prediction technique used to design the simulator. Also note that for $RGR \geq 40$ ft the first and second peaks are equal.

The calculated shock arrival times for the first and second static pressure peaks are included in Fig. 10. The arrival time difference between peaks grows rapidly for the first 30 feet up the ramp, and then remains constant at about $1 \text{ ms}/500T^{1/3}$. In addition, Fig. 10 depicts the Mach stem growth versus ramp ground range. The top of the Mach stem traces a path at an average angle of about 9 degrees above the ramp surface, which is consistent with shock tube data for square wave shock reflections from wedges (Ref. 7). Note that the Mach stem growth for the equivalent nuclear case is more rapid than in the case of the simulator.

Calculated static pressure histories are presented in Fig. 11 for various stations on the ramp ($34 \text{ ft} < RGR < 60 \text{ ft}$). The second peak dominates for $RGR < 34 \text{ ft}$, and then gradually melts into backside of the waveform. For $RGR > 60 \text{ ft}$, the second peak has essentially disappeared. Comparisons of static pressure histories at $h = 0, 1$ and 5.5 ft normal to the ramp for station 17 indicate that there is no vertical pressure gradient on the front end of the waveform.

Fig. 12 gives the calculated dynamic pressure histories on the ramp at stations corresponding to the static pressure histories of Fig. 11. At small ground ranges, the second peak dominates the first peak. The second peak decays in magnitude and duration as the Mach stem progresses up the ramp, and has essentially disappeared for $RGR > 60 \text{ ft}$. Comparisons of dynamic pressure histories at $h = 0, 1$ and 5.5 ft normal to the ramp for station 17 indicate very little vertical gradient for times less than 0.8 ms after shock arrival. However, the $h = 1 \text{ ft}$ station shows a strong second peak at about 1 ms which is absent from the $h = 0$ and 5 ft records. We believe that this is caused by a high density slug of gas at this altitude. A slip line (with high density material above and lower density material below) emanates from the triple point. As the slip line approaches the ramp it curls forward forming a region of high density fluid near the ramp surface ($h \sim 1 \text{ ft}/500T^{1/3}$) while the Mach stem at this station is about 10 ft high. This effect is similar to the contact surface rollup observed in numerical simulations of nuclear HOB detonations and square wave shock reflections from wedges (Ref. 9). This increase in dynamic pressure near the ramp can be very important to airblast loads on above ground

structures--it increases both the peak loads and the impulses to approximately $2 \text{ ms}/500T^{1/3}$.

Let us now relate the simulator environment to an equivalent nuclear height-of-burst case. Fig. 13 gives the ideal, nuclear peak overpressure HOB curves as constructed by H. J. Carpenter (Ref. 10). Region A corresponds to the regular reflection regime, and region B corresponds to the Mach reflection regime where the static pressure waveforms on the ground contain two peaks. In regions B_1 and B_2 , first and second peaks dominate, respectively. Along the dashed curve the first and second peaks are equal. Figure 9 indicates that for $30 \text{ ft} < \text{RGR} < 60 \text{ ft}$, first and second peaks are equal and range from 600 psi down to 400 psi. Figure 13 then indicates that for this range in pressure, the nuclear HOB parameters are the following:

$$\begin{aligned} 100 \text{ ft}/KT^{1/3} &\leq \text{HOB} \leq 120 \text{ ft}/KT^{1/3} \\ 190 \text{ ft}/KT^{1/3} &\leq \text{GR} \leq 210 \text{ ft}/KT^{1/3} \end{aligned}$$

Thus the simulator as analyzed in this report gives an airblast environment which is equivalent to a nuclear detonation at height-of-burst of about $110 \text{ ft}/KT^{1/3}$ and a ground range of about $200 \text{ ft}/KT^{1/3}$.

Finally, let us consider the effective yield of the simulator. A 500T high explosives surface burst produces a blast wave flow field which is equivalent to about a 1-KT nuclear surface burst (or a 2-KT nuclear free air burst). Nuclear static pressure waveforms in the 400 psi to 600 psi Mach reflection regime have double peaks with a time separation between peaks of about $2 \text{ ms}/KT_N^{1/3}$ (Ref. 10). The FAST2D calculation of the simulator flow field indicates a time separation between peaks of about $1 \text{ ms}/500T_{HE/SB}^{1/3}$, i.e., the time separation for the simulator is too small by a factor of about two. We believe that the time separation between peaks can be increased by making the Mach stem climb more rapidly. This can be accomplished by simultaneously decreasing the ramp angle and moving the ramp toward the charge.

V. SUMMARY AND CONCLUSIONS

Height-of-burst detonations create airblast environments and diffraction loads which are more severe than the surface burst case in the high overpressure Mach reflection regime. There is an ongoing need to simulate these HOB environments on a large scale to validate the survivability of military systems to blast effects. We propose using an existing high explosives test bed, say a 500T hemispherical charge,

to create the free field blast environment. A large ramp would be located near the charge. Shock diffraction on the ramp generates, in a rather natural way, a flow field which simulates the HOB blast environment with high fidelity.

A parametric analysis of such HOB simulators indicates that a 30° ramp situated about 200 feet from a 500T hemispherical charge would give useful environments. The flow field details near such a ramp were investigated with a 2-D hydrocode calculation. The calculation indicates that double peaked static and dynamic pressure waveforms were created near the ramp surface. In the 400 to 600 psi range, the calculated first and second static pressure peaks were equal. By use of the nuclear HOB curves, it was determined that the blast flow field corresponds to a nuclear detonation at a height-of-burst of 100 to 120 ft/ $KT_N^{1/3}$ and a ground range of 190 to 210 ft/ $KT_N^{1/3}$. Time separations between static pressure peaks were found to be about 1 ms/ $500T_{HE}^{1/3}$; this value was too small by about a factor of two for the nuclear case.

VI. RECOMMENDATIONS

Additional analysis should be performed to refine the HOB simulator design. The 2-D hydrocode simulations are quite useful because they allow one to examine the entire flow field in a non-interfering way. An improvement is needed on the boundary condition modeling of the ramp--the stairstep model gave very noisy results on the ramp surface. Small charge (say 4-lb hemispherical PBX-9404 charges) tests can provide an experimental definition of the blast environment. Ramp angle, location and surface curvature could be varied parametrically in such tests. Pressure gauges on the ramps can measure static pressure histories with high fidelity, while shadowgraph photography can capture the shock structure on the ramp. These results could be used to design a simulator which, we suggest, should be fielded on the next 500T HE test.

ACKNOWLEDGMENTS

We would like to acknowledge the contributions of H. J. Carpenter in this work. In July of 1980, he and one of the authors (A. Kuhl) first postulated the idea that a large ramp, in conjunction with an HE charge, could be used to simulate HOB environments on a large scale. His careful critique of the manuscript and his stimulating discussions on this subject are greatly appreciated.

This work was sponsored by the Defense Nuclear Agency under Contract Number DNA001-81-C-0023. Dr. George Ullrich was project officer for this effort.

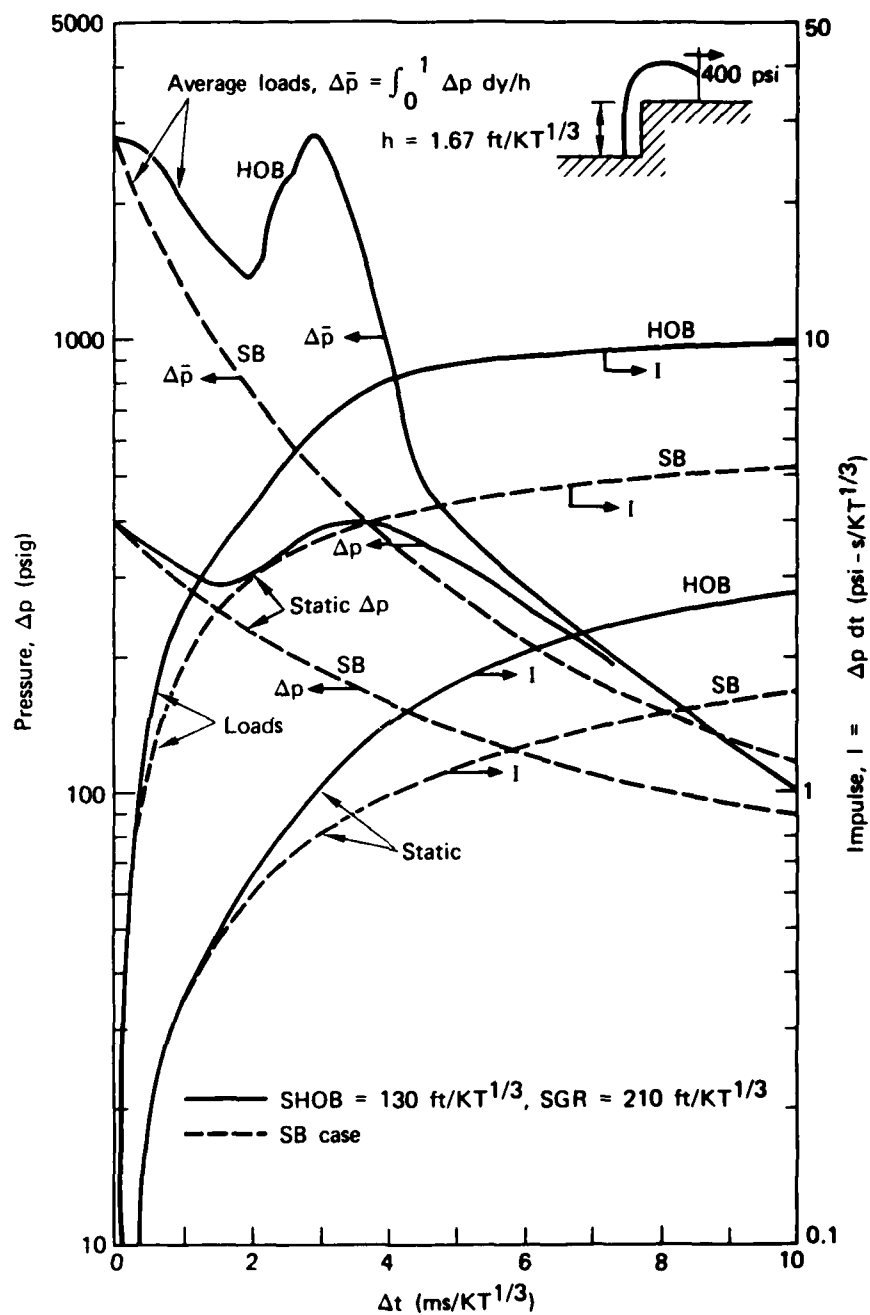


Fig. 1 — Comparison of nuclear surface burst and height-of-burst loads and impulses at the 400-psi station

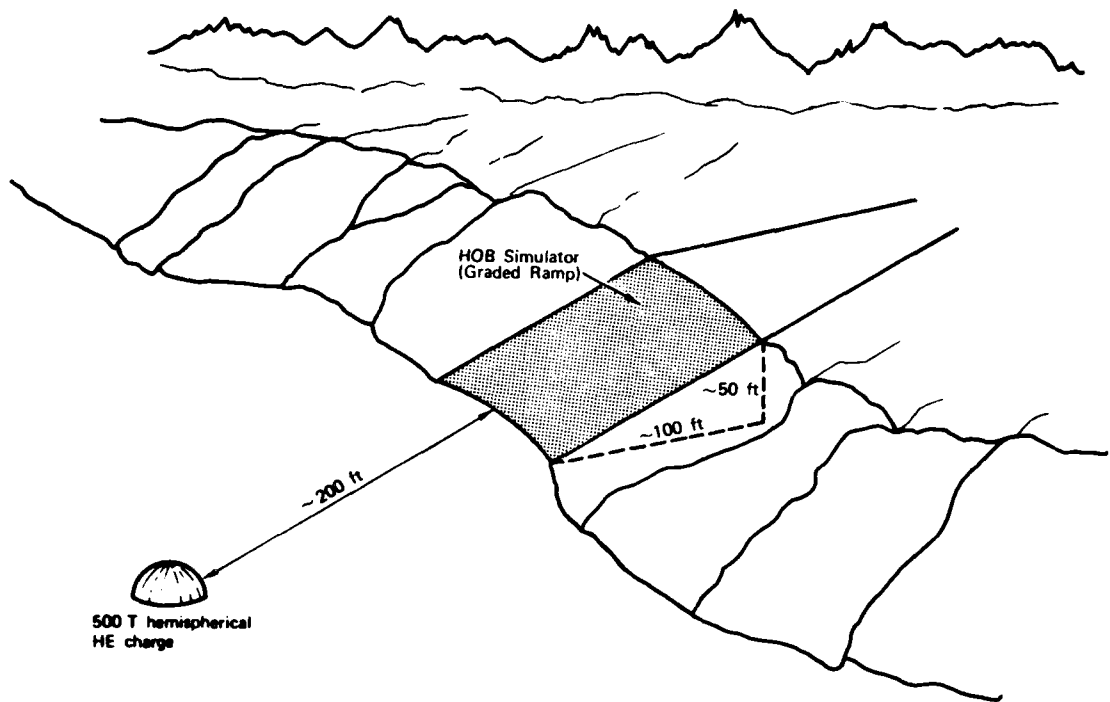


Fig. 2 — HOB simulator concept (graded ramp) on a large-scale HE test

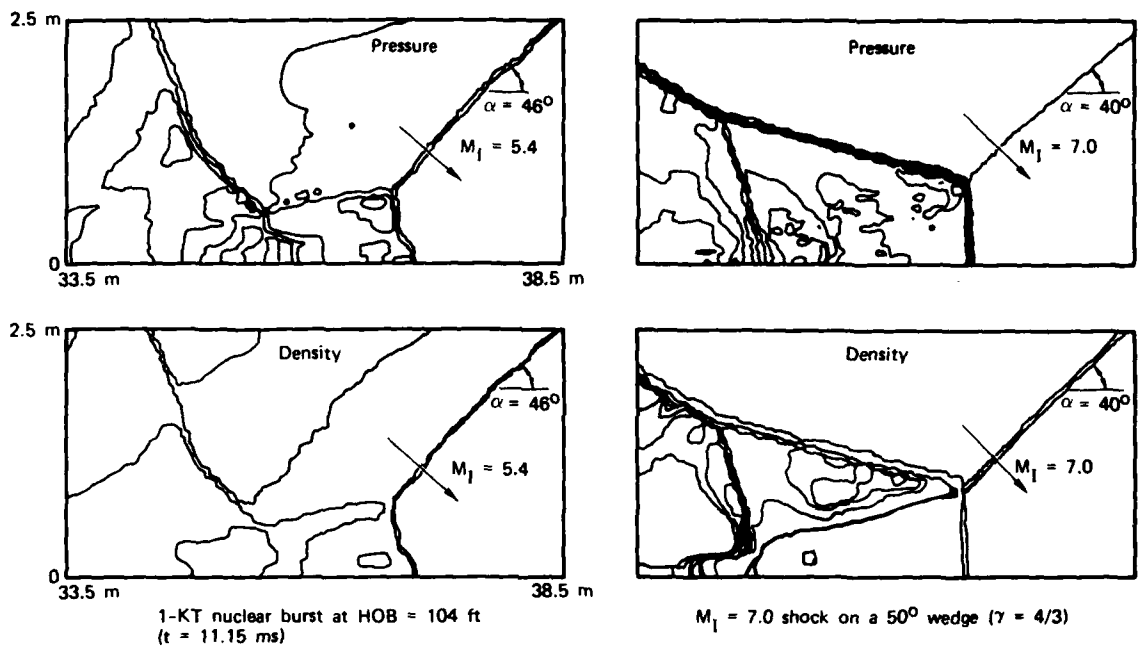


Fig. 3 — Comparison of calculated pressure and density contours for a nuclear HOB case and a square wave shock on a wedge

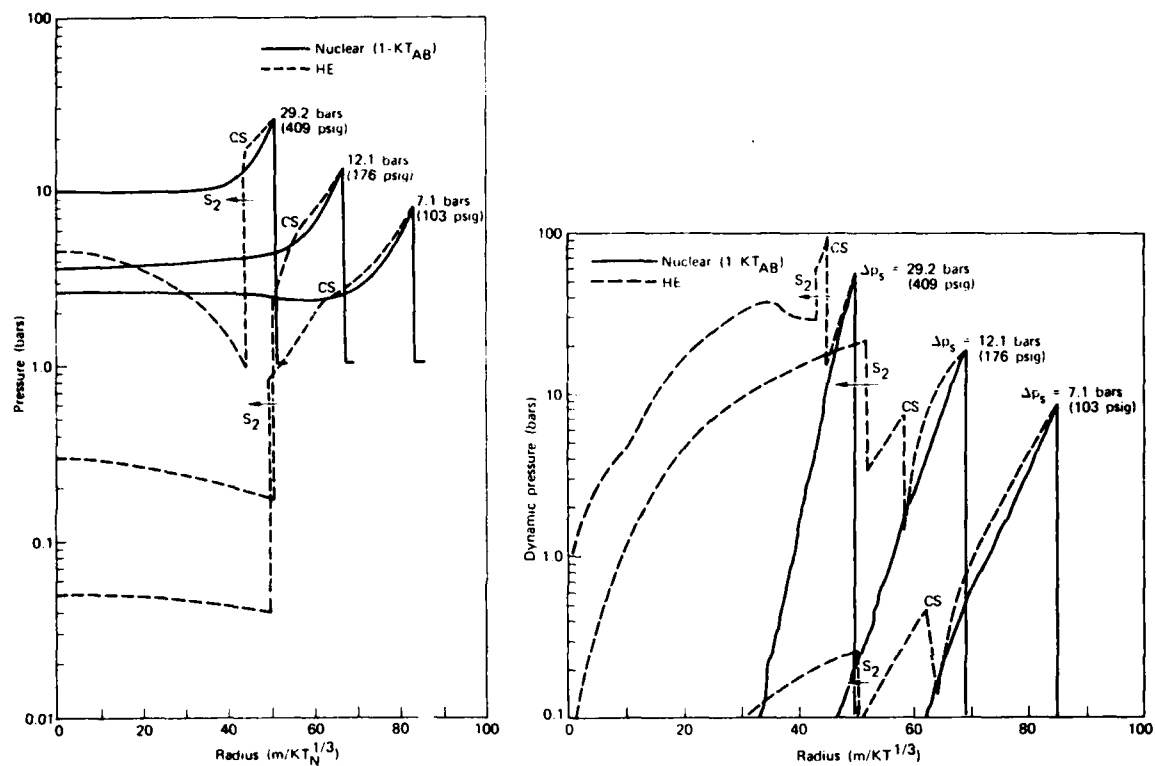


Fig. 4 — Comparison of HE and nuclear free-air burst static and dynamic pressure waveforms at shock overpressures ~ 100, 200, and 400 psi

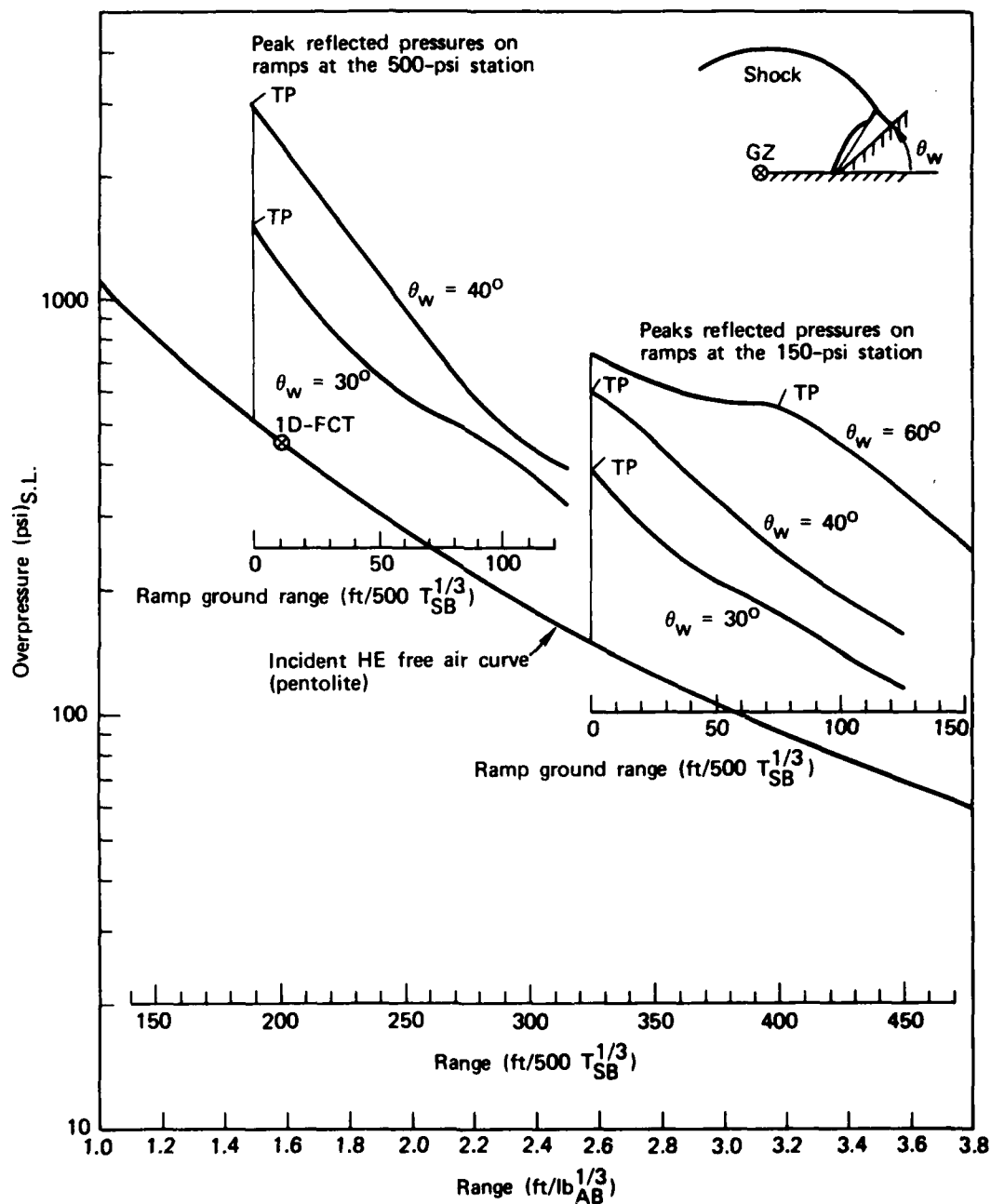


Fig. 5 — Parametric results of peak reflected pressures on the ramp HOB simulator

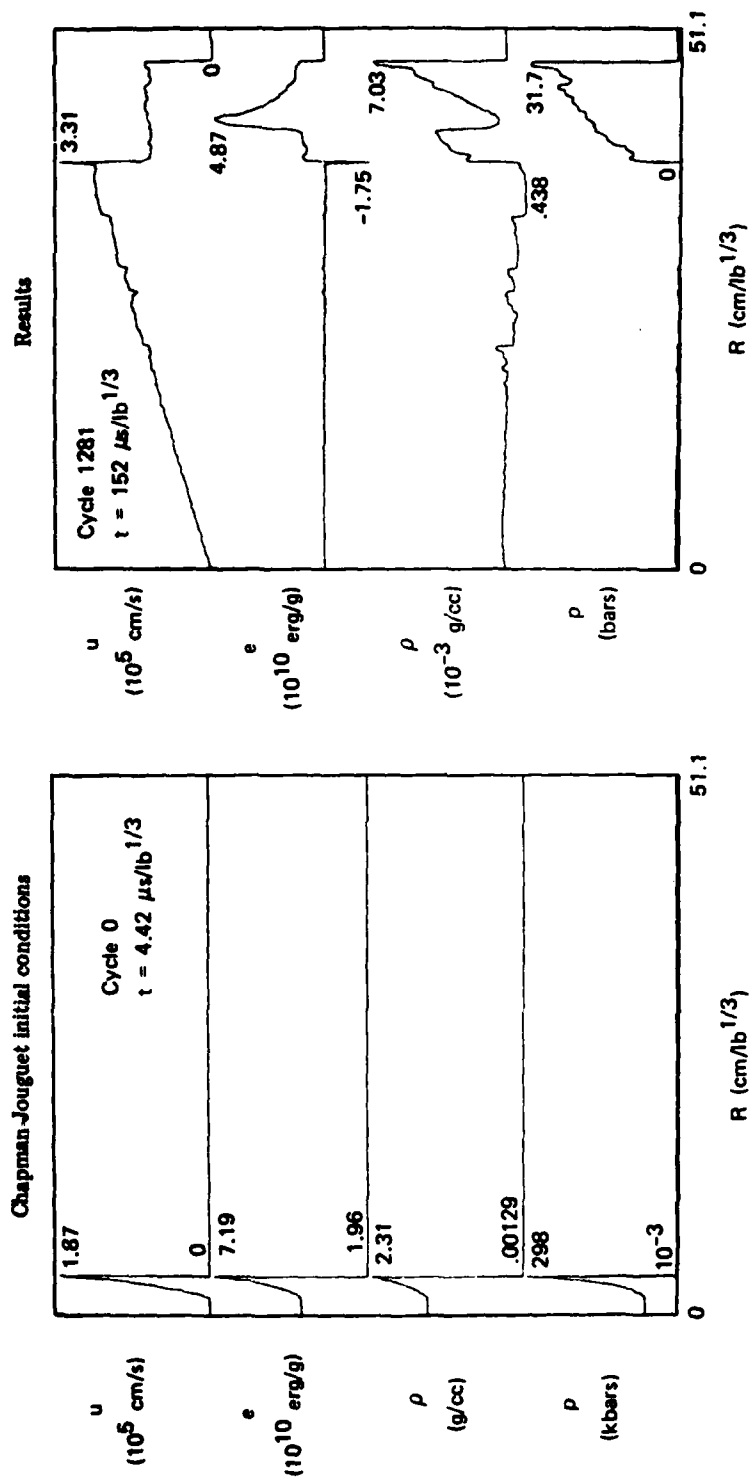


Fig. 6 — Calculated 1-D flow field distribution of a spherical 1-lb PBX-9404 charge
 $(\Delta r = 0.1025 \text{ cm}, 500 \text{ cells, real air and JWL EOS})$

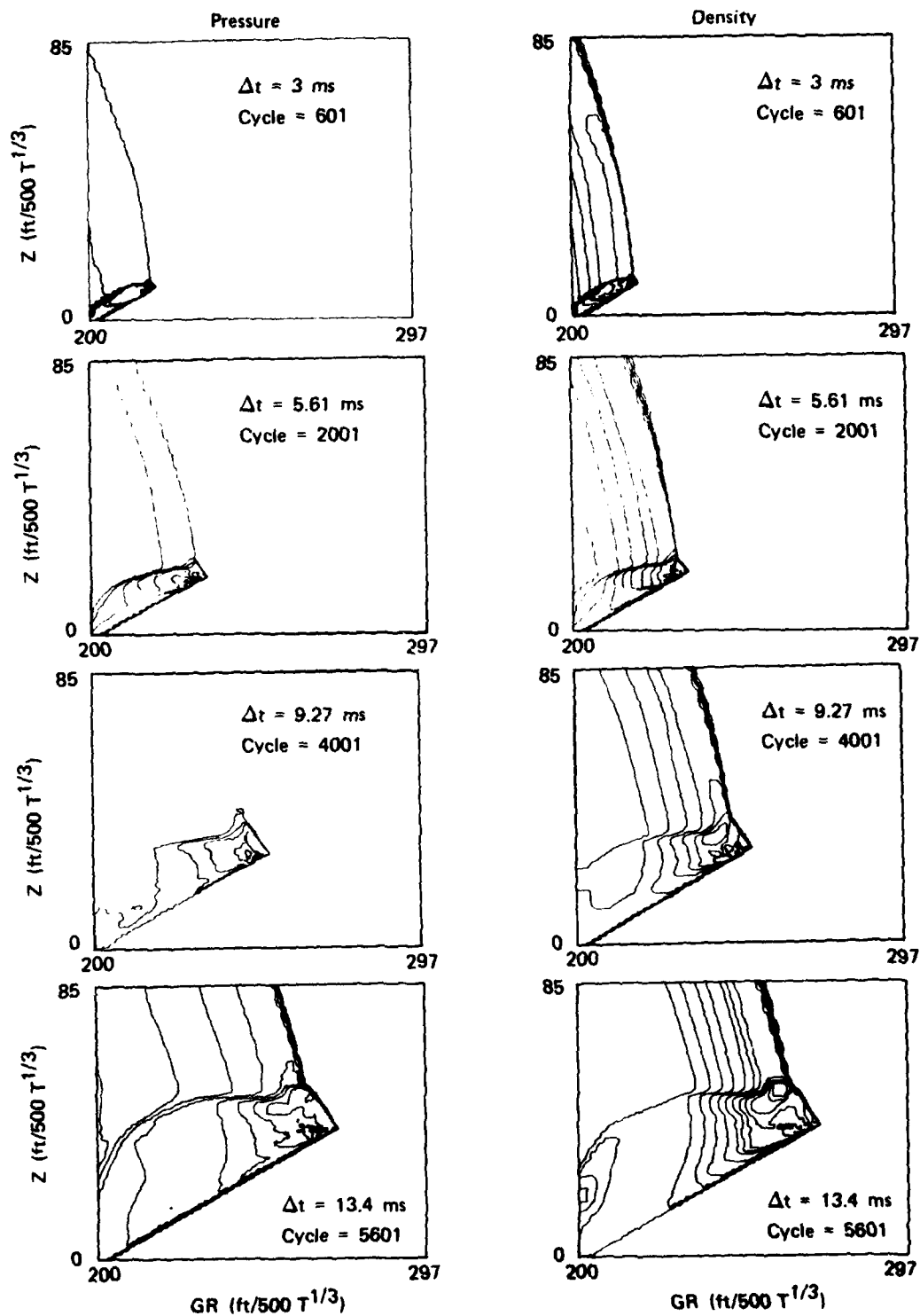


Fig. 7 — Calculated pressure and density contours at times $\Delta t = 3.0, 5.61, 9.27$, and 13.4 ms/500 $T^{1/3}$ ($t_0 = 19.2$ ms/500 $T^{1/3}$)

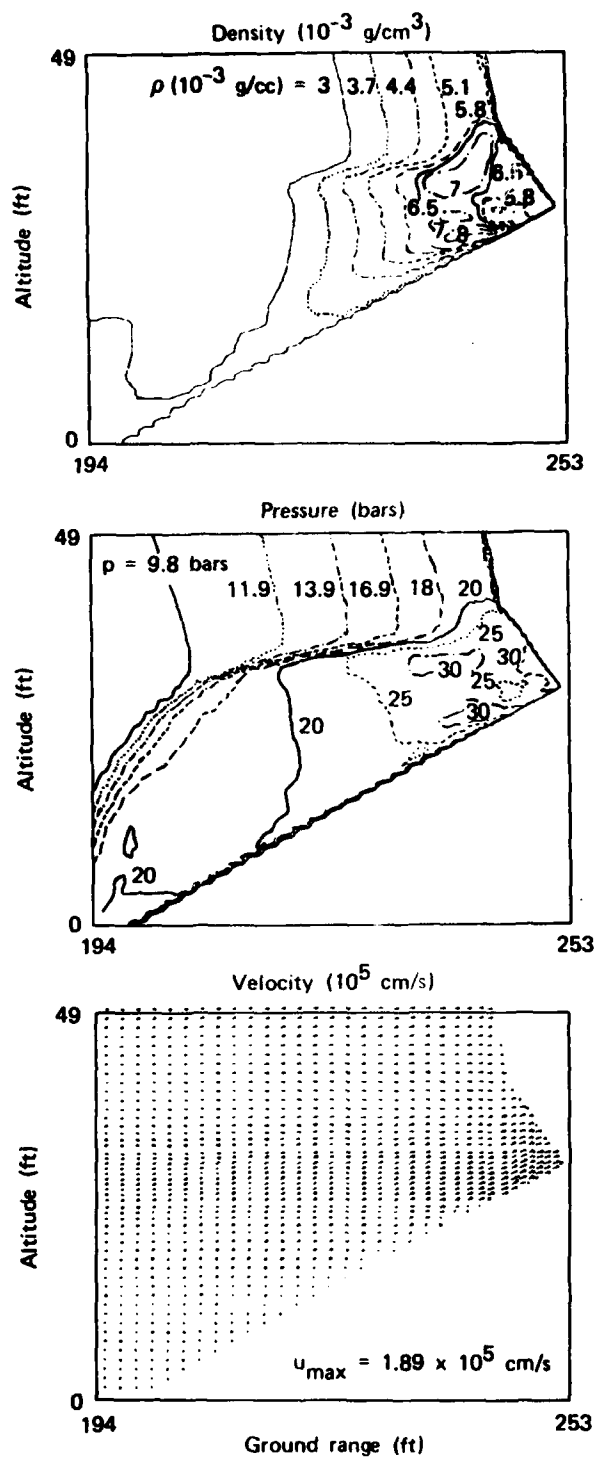


Fig. 8 — Calculated flow details at $\Delta t = 9.61 \text{ ms}/500 T^{1/3}$

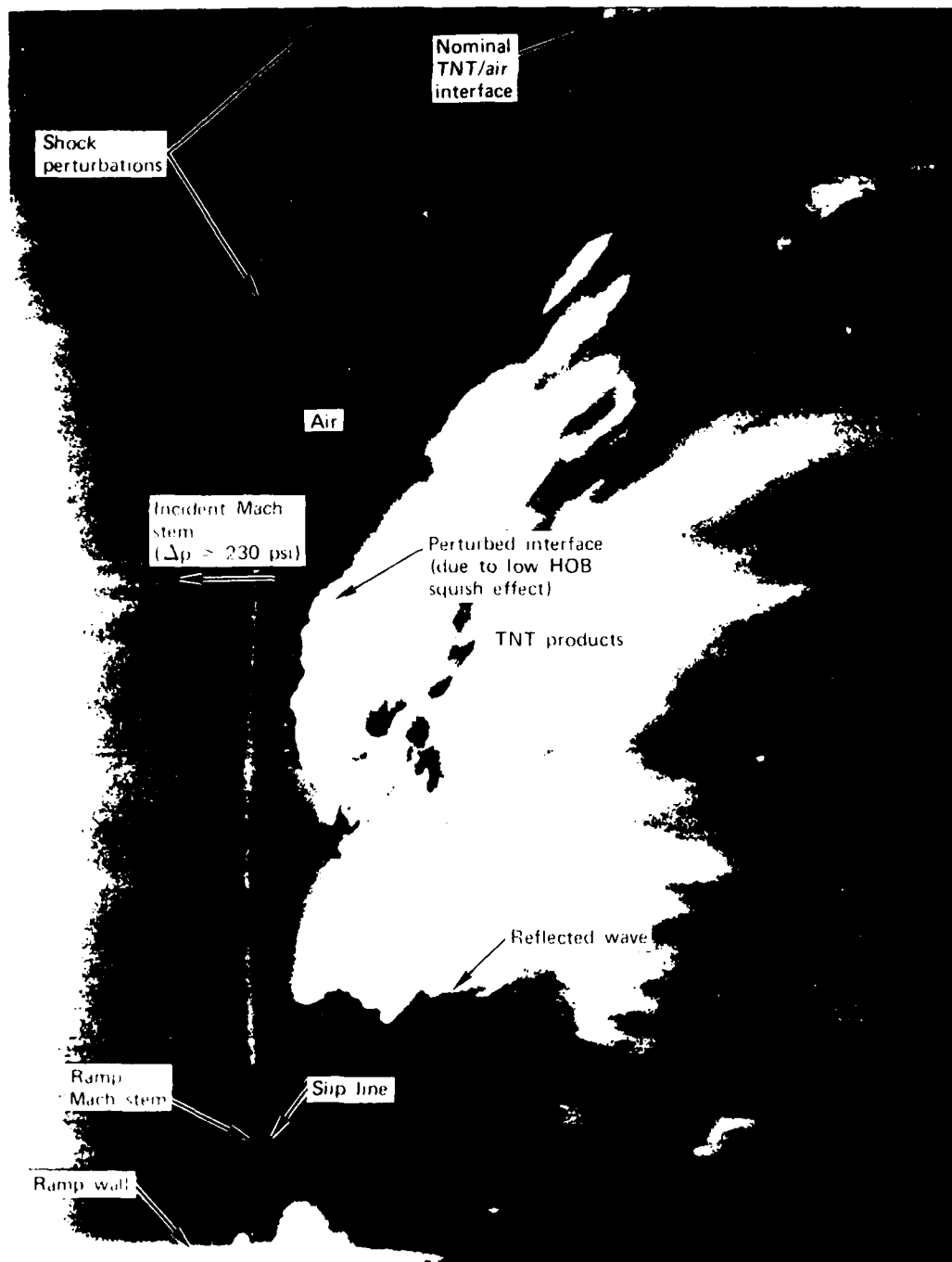


Fig. 9 — Shadowgraph of the shock wave structure formed by an 8-lb TNT-driven blast wave ($HOB = 1.04 \text{ ft/lb}^{1/3}$) diffracting on a 31° ramp; incident pressure at the beginning of the ramp was about 120 psi. (Courtesy of W. F. Dudziak, Information Science, Inc.)

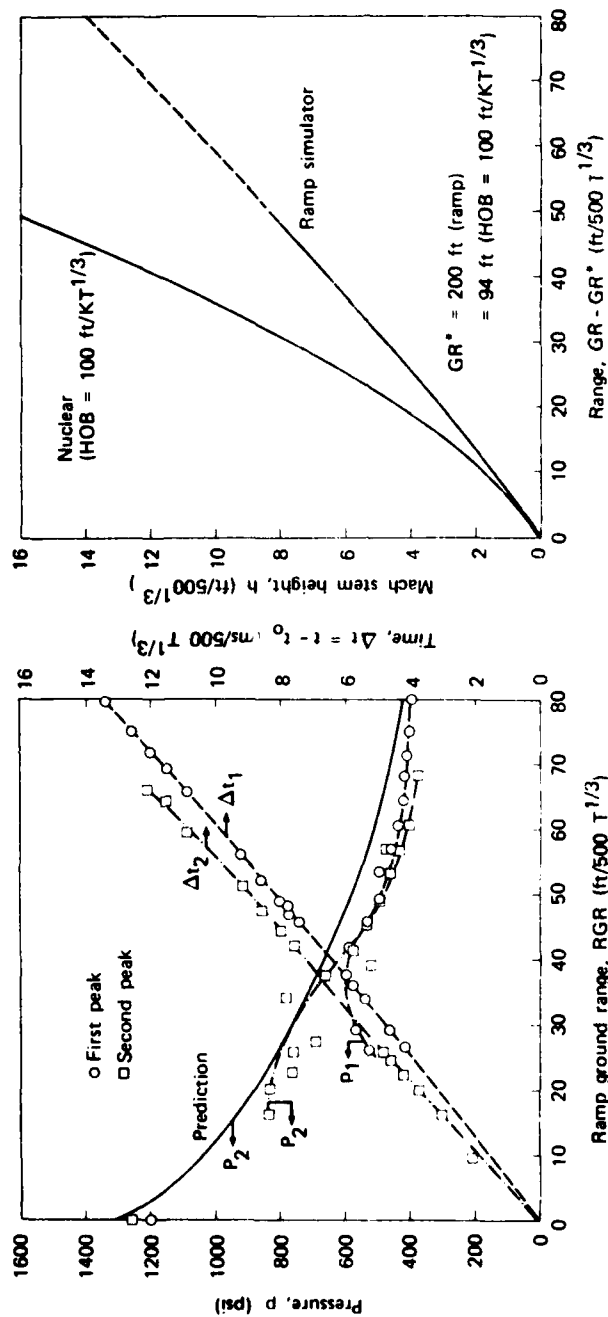


Fig. 10 — Calculated peak pressure, shock arrival time and Mach stem height vs ground range for the ramp HOB simulator ($GR_{\text{ramp}} = 200 \text{ ft}/500 T^{1/3}$, $t_0 = 19.2 \text{ ms}/500 T^{1/3}$).

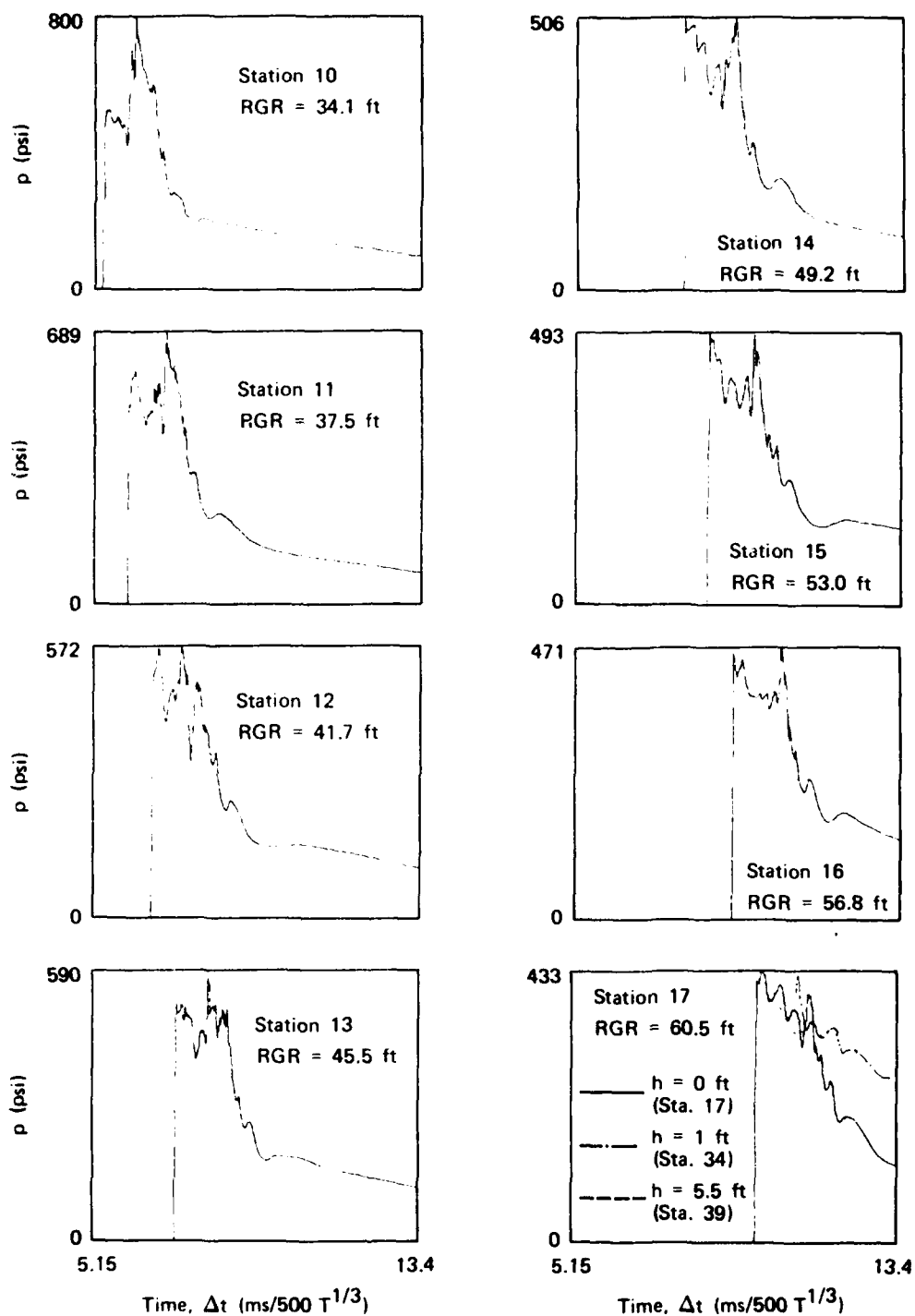


Fig. 11 — Calculated static pressure time histories at various stations on the ramp ($t_0 = 19.2$ ms/500 $T^{1/3}$)

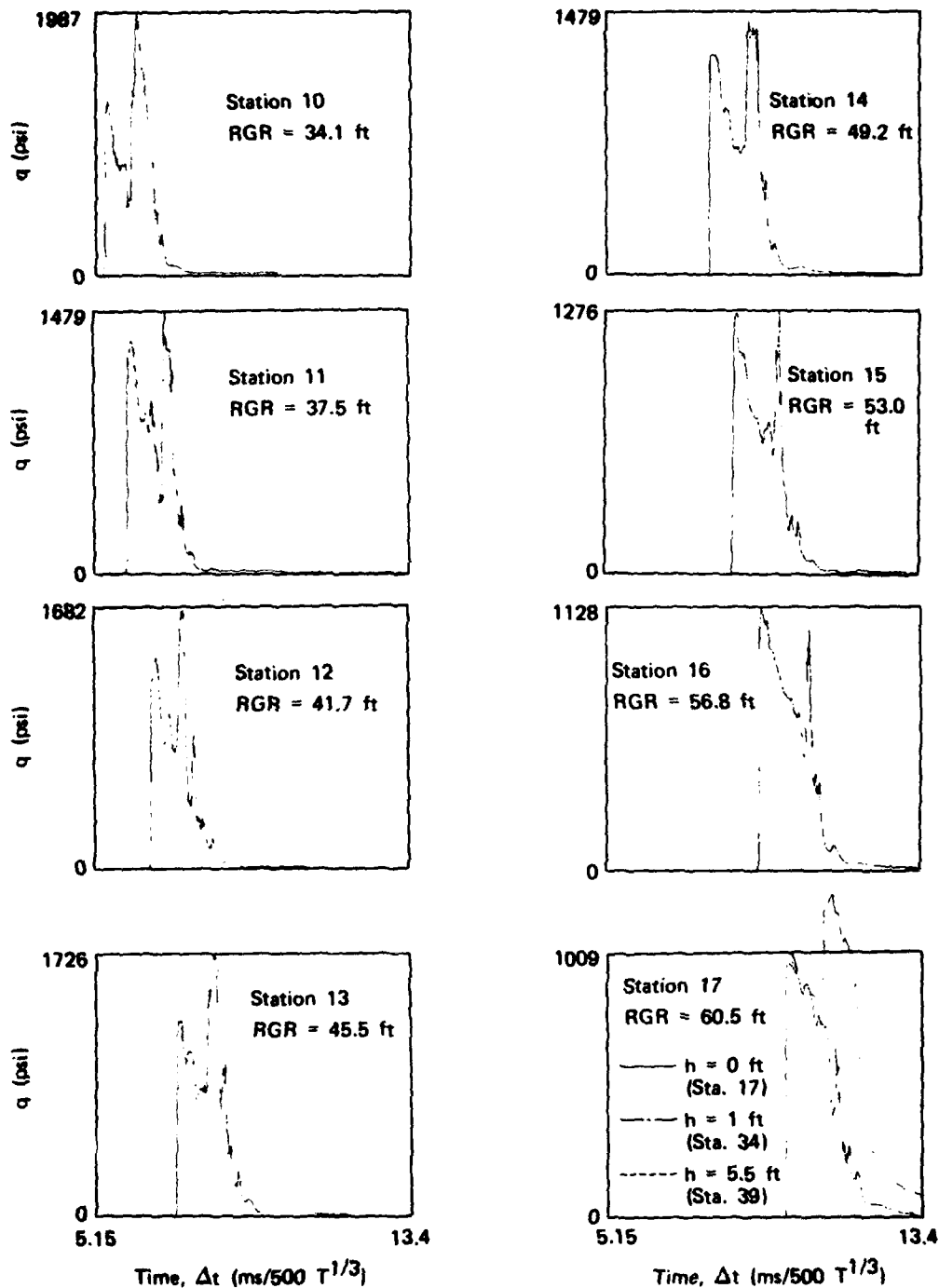


Fig. 12 — Calculated dynamic pressure time histories at various stations on the ramp ($t_0 = 19.2$ ms/500 $T^{1/3}$)

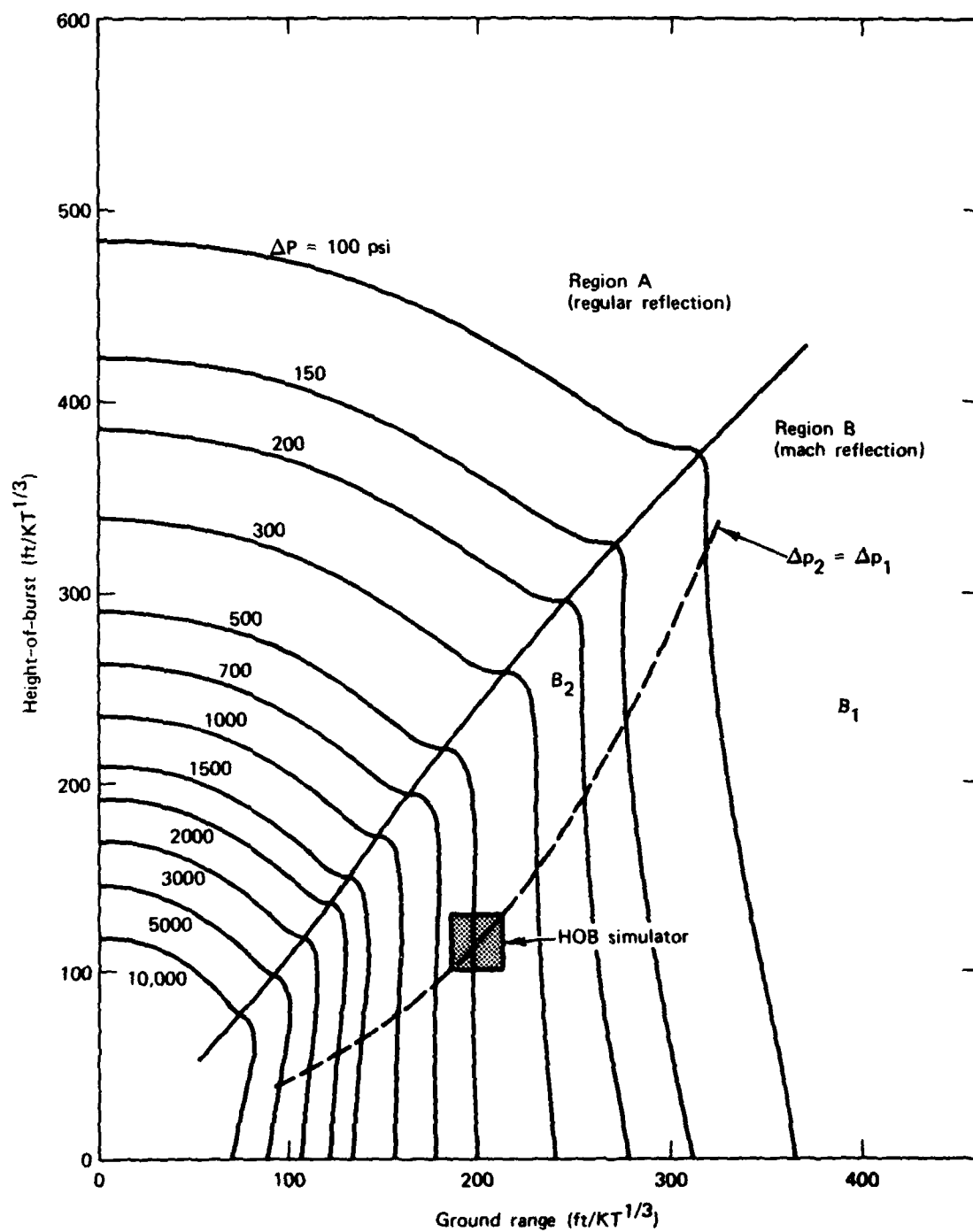


Fig. 13 — Ideal nuclear peak overpressure height-of-burst curves (Ref. 10)

REFERENCES

1. Carpenter, H. J., "Height-of-Burst Blast at High Overpressure," 4th Int. Symposium on Military Applications of Blast Simulation, (1974).
2. Keefer, J. and Reisler, R., U. S. Ballistic Research Laboratory, (private communication, 1979).
3. Brode, H. L., A Calculation of the Blast Wave from a Spherical Charge of TNT, Rand Report RM-1965 (1957).
4. Brode, H. L., Theoretical Description of the Blast and Fireball for a Sea-Level Kiloton Explosion (U), Rand Report RM-2246-PR (1966).
5. Boris, J. P., Flux-Corrected Transport Algorithms for Solving Generalized Continuity Equations, NRL Report 3237 (1976).
6. Kuhl, A. L., Seizew, M. R., Analysis of Ideal, Strong, Chapman-Jouguet Detonations, TRW Report 78.4735.9-13 (1978).
7. Ben-Dor, G., Glass, I. I., "Domains and Boundaries of Non-stationary Oblique Shock-Wave Reflections: 1. Diatomic Gas," J. Fluid Mechanics, Vol. 92, Pt. 3, pp. 459-496 (1979).
8. Dudziak, W. F., Information Science, Inc. (private communication, May 9, 1981).
9. Book, D., Boris, J., Kuhl, A., Oran, E., Picone, M., Zalesak, S., "Simulation of Complex Shock Reflections from Wedges in Inert and Reactive Gaseous Mixtures," Seventh Int. Conference on Numerical Methods in Fluid Dynamics, Springer-Verlag (1981).
10. Carpenter, H. J., RDA (private communication, 1979).

DISTRIBUTION LIST

DEPARTMENT OF DEFENSE

ASSISTANT TO THE SECRETARY OF DEFENSE
(ATOMIC ENERGY)
WASHINGTON, DC 20301
OICV ATTN EXECUTIVE ASSISTANT

DIRECTOR
DEFENSE COMMUNICATIONS AGENCY
WASHINGTON, DC 20305
(APP CODES: ATTN CODE 240 FOR)
OICV ATTN CODE 672 S LIPP

DIRECTOR
DEFENSE INTELLIGENCE AGENCY
WASHINGTON, DC 20301
OICV ATTN PDS-3A (TECH LIP)
OICV ATTN DB 4N
OICV ATTN DT 1C
OICV ATTN DT-2
OICV ATTN DB 4C F DEARRELL

DIRECTOR
DEFENSE NUCLEAR AGENCY
WASHINGTON, DC 20305
OICV ATTN SPSS
OICV ATTN SPSS G ULIRICH
OICV ATTN SPSS T DEEVY
OICV ATTN TITI

DEFENSE TECHNICAL INFORMATION CENTER
CAMERON STATION
ALEXANDRIA, VA 22304
(12 IF OPEN PUB, OTHERWISE 2 - NO UNINTL)
OICV ATTN DT

CHAIRMAN
DEPARTMENT OF DEFENSE EXPLO SAFETY BOARD
HOFFMAN BLDG 1, RM 856-C
2441 EISENHOWER AVENUE
ALEXANDRIA, VA 22301
OICY ATTN CHAIRMAN

COMMANDER
FIELD COMMAND
DEFENSE NUCLEAR AGENCY
KIRTLAND AFB, NM 87115
OICY ATTN ECXOF
OICY ATTN ECT
OICY ATTN ECPB
OICY ATTN ECTT

CHIEF
FIELD COMMAND
DEFENSE NUCLEAR AGENCY
LIVERMORE BRANCH
20 BOX 808 L-217
LIVERMORE, CA 94550
OICY ATTN ECPPL

DEFECON
JOINT STRAT TGT PLANNING STAFF
OFFUTT AFB
OMAHA, NB 68113
OICY ATTN JLA
OICY ATTN JOXT
OICY ATTN YDES
OICY ATTN M21-STRINFO LIBRARY
OICY ATTN JUTW-2

COMMANDANT
NATO SCHOOL (SHAPE)
APO NEW YORK 09172
OICY ATTN U.S. DOCUMENTS OFFICER

UNDER SECY OF DEF FOR RSCH & ENGRG
DEPARTMENT OF DEFENSE
WASHINGTON, DC 20301
OICY ATTN STRATEGIC & SPACE SYS (CS) RM 35120

DEPARTMENT OF THE ARMY

DIRECTOR
BMD ADVANCED TECHNOLOGY CENTER
DEPARTMENT OF THE ARMY
P O BOX 1500
HUNTSVILLE, AL 35807
OICY ATTN ATC-T
OICY ATTN ICRDABH-X
OICY ATTN ATC-T

COMMANDER
BMD SYSTEMS COMMAND
DEPARTMENT OF THE ARMY
P O BOX 1500
HUNTSVILLE, AL 35807
OICY ATTN BMDSC-FW
OICY ATTN BMDSC-HW P DEKALB
OICY ATTN BMDSC-H N HURST
OICY ATTN BMDSC - R.C. WEBB

CHIEF OF ENGINEERS
DEPARTMENT OF THE ARMY
FORRESTAL BUILDING
WASHINGTON, DC 20314
OICY ATTN DAEN-MCE-D
OICY ATTN DAEN-RDL
OICY ATTN DAEN-MPE-T D PEYNOLDS

DEP CH OF STAFF FOR OPS & PLANS
DEPARTMENT OF THE ARMY
WASHINGTON, DC 20310
OICY ATTN DAMC-NC

COMMANDER
HARRY DIAMOND LABORATORIES
DEPARTMENT OF THE ARMY
2800 POWDER MILL ROAD
ADELPHI, MD 20783
(CNVOT- INNER ENVELOPE: ATTN: DELHD-RBH ECR)
OICY ATTN DELHD-I-TL (TECH LIR)
OICY ATTN CHIEF DIV 20700

COMMANDER
U S ARMY ARMAMENT MATERIAL READINESS COMMAND
ROCK ISLAND, IL 61207
OICV ATTN MA LIBRARY

DIRECTOR
U S ARMY BALLISTIC RESEARCH LABS
ABERDEEN PROVING GROUND, MD 21075
OICV ATTN OPDAP-BLV
OICV ATTN OPDAP-BLT J KEEFER
OICV ATTN OPDAP-TSP-S (TECH LIB)

COMMANDER AND DIRECTOR
U S ARMY COLO REGION RES ENGR LAB
P O BOX 242
HANOVER, NH 03755
OICV ATTN LIBRARY

COMMANDER
U S ARMY CONCEPTS ANALYSIS AGENCY
9120 WOODMONT AVENUE
PETHESDA, MD 20014
OICV ATTN CSSA-ADL (TECH LIB)

DIRECTOR
U S ARMY CONSTRUCTION ENGRG RES LAB
P O BOX 4005
CHAMPAIGN, IL 61820
OICV ATTN LIBRARY

COMMANDER
U S ARMY ENGINEER CENTER
FORT BELVOIR, VA 22060
OICV ATTN TECHNICAL LIBRARY
OICV ATTN ATTA

DIVISION ENGINEER
U S ARMY ENGINEER DIV HUNTSVILLE
P O BOX 1600, WEST STATION
HUNTSVILLE, AL 35907
OICV ATTN HVED-SP
ATTN HVED-ED

DIRECTOR
U S ARMY ENGR WATERWAYS EXPR STATION
P O BOX 631

VICKSBURG, MS 39180

OICY ATTN J ZELASKO
OICY ATTN WESSO J JACKSON
OICY ATTN J STRANGE
OICY ATTN WESSE L INGRAM
OICY ATTN LIBRARY
OICY ATTN WESSA W FLATHAU

COMMANDER
U S ARMY FOREIGN SCIENCE & TECH CTR
220 7TH STREET, NE
CHAPEL HILL, VA 22901
OICY ATTN DRXST SE

COMMANDER
U S ARMY MATERIAL & MECHANICS RSCH CTR
WATERLOO, MA 02172
(ADDRESS CNWDI: ATTN: DOCUMENT CONTROL FOR:)
OICY ATTN TECHNICAL LIBRARY
OICY ATTN DRYNR-TE R SHEA
OICY ATTN DRXNR J MESSALL

COMMANDEE
U S ARMY MATERIAL DEV & READINESS CMD
5001 EISENHOWER AVENUE
ALEXANDRIA, VA 22332
OICY ATTN DRCD-ED L FLYNN
OICY ATTN DRYAM-IL (TECH LIO) UNCL ONLY

COMMANDER
U S ARMY MISSILE COMMAND
REDSTONE ARSENAL, AL 35899
OICV ATTN PSIC
OICV ATTN DDDMI-XS

COMMANDER
U S ARMY MOBILITY EQUIP REG CYS
FORT BELVOIR, VA 22060
(CONVICT TO ARMY MAT DEV & READINESS COMMAND)
OICV ATTN DDDME-WC (TECH LIB)

COMMANDER
U S ARMY NUCLEAR & CHEMICAL AGENCY
7500 BACKLICK ROAD
BUILDING 2073
SPRINGFIELD, VA 22150
(DESIRES ONLY 1 CY TO LIBRARY)
OICV ATTN J SIMMS
OICV ATTN LIBRARY

COMMANDANT
U S ARMY WAR COLLEGE
CARLISLE BARRACKS, PA 17012
OICV ATTN LIBRARY

DEPARTMENT OF NAVY

COMMANDER
DAVID TAYLOR NAVAL SHIP R E D CTR
BETHESDA, MD 20084
(CONVDT ONLY ATTN MRS. M. BIRKHEAD CODE 5815.6)
OICV ATTN CODE 142-3 (LIBRARY)

OFFICER-IN-CHARGE
NAVAL CIVIL ENGINEERING LABORATORY
PORT HUENEME, CA 93041
OICV ATTN CODE 152 J FORREST
OICV ATTN CODE LCRA (LIBRARY)
OICV ATTN CODE 151 J CRAWFORD
OICV ATTN 151 R MURTHA

COMMANDER
NAVAL ELECTRONIC SYSTEMS COMMAND
WASHINGTON, DC 20360
OICV ATTN PMS 117-21

COMMANDER
NAVAL FACILITIES ENGINEERING COMMAND
WASHINGTON, DC 20360
OICV ATTN CODE 040

HEADQUARTERS
NAVAL MATERIAL COMMAND
WASHINGTON, DC 20360
OICV ATTN MAT 08T-22

COMMANDER
NAVAL OCEAN SYSTEMS CENTER
SAN DIEGO, CA 92152
OICY ATTN CODE 213 E COOPER
OICY ATTN CODE 4471 (TECH LIB)

SUPERINTENDENT
NAVAL POSTGRADUATE SCHOOL
MONTEREY, CA 93940
(DESIRES NO CNWDI DOCUMENTS)
OICY ATTN CODE 1424 LIBRARY
OICY ATTN G LINDSAY

COMMANDING OFFICER
NAVAL RESEARCH LABORATORY
WASHINGTON, DC 20375
(RD & RD/M ATTN CODE 1221 FOR & RD ATTN CODE 2628 FOR)
OICY ATTN CODE 4040 J BORIS
OICY ATTN CODE 2627 (TECH LIB)
OICY ATTN CODE 4040 D BOCK

COMMANDER
NAVAL SEA SYSTEMS COMMAND
WASHINGTON, DC 20362
OICY ATTN SEA-00652 (LIB)
OICY ATTN SEA-0351

OFFICER IN CHARGE
NAVAL SURFACE WEAPONS CENTER
WHITE OAK LABORATORY
SILVER SPRING, MD 20910
OICY ATTN R44 H CLAZ
OICY ATTN CODE F21
OICY ATTN CODE X211 (TECH LIB)

COMMANDER
NAVAL SURFACE WEAPONS CENTER
DAHLGREN, VA 22449
OICV ATTN TECH LIBRARY & INFO SVCS BR

PRESIDENT
NAVAL WAR COLLEGE
NEWPORT, RI 02840
OICV ATTN CODE E-11 (TECH SERVICE)

COMMANDER
NAVAL WEAPONS CENTER
CHINA LAKE, CA 92555
OICV ATTN CODE 2201 P COPPLE
OICV ATTN CODE 266 C AUSTIN
OICV ATTN CODE 223 (TECH LIB)

COMMANDING OFFICER
NAVAL WEAPONS EVALUATION FACILITY
KIRTLAND AIR FORCE BASE
ALBUQUERQUE, NM 87117
OICV ATTN R HUGHES
OICV ATTN CODE 10 (TECH LIB)

OFFICE OF NAVAL RESEARCH
ARLINGTON, VA 22217
OICV ATTN CODE 674 N PERONE

OFFICE OF THE CHIEF OF NAVAL OPERATIONS
WASHINGTON, DC 20350
OICV ATTN OP 581
OICV ATTN OP 0350

DIRECTOR
STRATEGIC SYSTEMS PROJECT OFFICE
DEPARTMENT OF THE NAVY
WASHINGTON, DC 20376
OICV ATTN NSP-272
OICV ATTN NSP-42 (TECH LIB)

DEPARTMENT OF THE AIR FORCE

AIR FORCE GEOPHYSICS LABORATORY
HANSCOM AFB, MA 01731
OICY ATTN L W K THOMPSON

AIR FORCE INSTITUTE OF TECHNOLOGY
AIR UNIVERSITY
WRIGHT-PATTERSON AFB, OH 45433
(DOES NOT DESIRE CLASSIFIED DOCUMENTS)
OICY ATTN LIBRARY

HEADQUARTERS
AIR FORCE SYSTEMS COMMAND
ANDREWS AFB, DC 20334
OICY ATTN OLM
OICY ATTN OLM

AIR FORCE WEAPONS LABORATORY, AFSC
KENTLAND AFB, NM 87117
OICY ATTN NITES-C R HEAVY
OICY ATTN NITES-I
OICY ATTN NITES-C MATAHUCCI
OICY ATTN NITES-M PLAMONDON
OICY ATTN NITES-P DAYTON
OICY ATTN NITES-A
OICY ATTN NITES-G
OICY ATTN SUL
OICY ATTN DEY
OICY ATTN NITES-S
OICY ATTN NITES
OICY ATTN DEY

DIRECTOR
AIR UNIVERSITY LIBRARY
DEPARTMENT OF THE AIR FORCE
MAXWELL AFB, AL 36112
(DESIGNS NO (NWDI))
OICY ATTN AUL-1SE

ASSISTANT CHIEF OF STAFF
INTELLIGENCE
DEPARTMENT OF THE AIR FORCE
WASHINGTON, DC 20330
OICY ATTN IN RM 4A932

ASSISTANT CHIEF OF STAFF
STUDIES & ANALYSES
DEPARTMENT OF THE AIR FORCE
WASHINGTON, DC 20330
OICY ATTN AF/SAMI (TECH LIB)

ASSISTANT SECRETARY OF THE AF
RESEARCH, DEVELOPMENT & LOGISTICS
DEPARTMENT OF THE AIR FORCE
WASHINGTON, DC 20330
OICY ATTN SAFAIR/DEP FOR STRAT & SPACE SYS

BALLISTIC MISSILE OFFICE/MN
AIR FORCE SYSTEMS COMMAND
NORTON AFB, CA 92409
(MINUTEMAN)
OICY ATTN MNXXH G KALANSKY
OICY ATTN MNXXH M DELVECCHIO
OICY ATTN MN W GRABTREE
OICY ATTN MNXXH D GAGE
OICY ATTN MNXXH

DEPUTY CHIEF OF STAFF
RESEARCH, DEVELOPMENT, & ACC
DEPARTMENT OF THE AIR FORCE
WASHINGTON, DC 20330
OICY ATTN AFDDOI N ALEXANDROW
OICY ATTN AFDDPN
OICY ATTN AFDDOI

DEPUTY CHIEF OF STAFF
LOGISTICS & ENGINEERING
DEPARTMENT OF THE AIR FORCE
WASHINGTON, DC 20330
OICY ATTN LEEF

COMMANDER
FOREIGN TECHNOLOGY DIVISION, AFSC
WRIGHT-PATTERSON AFB, OH 45433
OICY ATTN THIS LIBRARY

COMMANDER
ROME AIR DEVELOPMENT CENTER, AFSC
GRIFFISS AFB, NY 13441
(CESIDES NC CNUOT)
OICY ATTN ISLC

STRATEGIC AIR COMMAND
DEPARTMENT OF THE AIR FORCE
OFFUTT AFB, NE 68112
OICY ATTN NSI-STINFC LIBRARY
OICY ATTN XPFS
OICY ATTN INT J MONTANECY

VELA SEISMOLOGICAL CENTER
312 MONTGOMERY STREET
ALEXANDRIA, VA 22314
OICY ATTN GUILPICH

DEPARTMENT OF ENERGY/OGE CONTRACTORS

DEPARTMENT OF ENERGY
ALBUQUERQUE OPERATIONS OFFICE
P O BOX 5400
ALBUQUERQUE, NM 87115
OICY ATTN CTID

DEPARTMENT OF ENERGY
WASHINGTON, DC 20545
OICY ATTN CHA/PCBT

DEPARTMENT OF ENERGY
NEVADA OPERATIONS OFFICE
P O BOX 14100
LAS VEGAS, NV 89114
OICY ATTN MAIL & RECORDS FOR TECHNICAL LIBRARY

LAWRENCE LIVERMORE NATIONAL LAB
P O BOX 808
LIVERMORE, CA 94550
OICY ATTN L-200 R DONG
OICY ATTN L 205 J HEARST (CLASS L-203)
OICY ATTN L 90 D MORRIS (CLASS L-504)
OICY ATTN L-7 J KAHN
OICY ATTN D GLENN
OICY ATTN L 427 R SCHECK
OICY ATTN TECHNICAL INFO DEPT. LIBRARY
OICY ATTN L-200 T BLTKOVICH

LOS ALAMOS NATIONAL SCIENTIFIC LAB
MAIL STATION 5000
P O BOX 1663
LOS ALAMOS, NM 87545
(CLASSIFIED ONLY TO MAIL STATION 5000)
OICY ATTN P WHITTAKER
OICY ATTN C KELLER
OICY ATTN M.T. SANFORD
OICY ATTN MS 364 (CLASS REPORTS LIB)
OICY ATTN E. JONES

LOVELACE BIOMEDICAL &
ENVIRONMENTAL PSCH INSTITUTE, INC.
P O BOX 5890
ALBUQUERQUE, NM 87115
OICV ATTN P JONES (UNCL ONLY)

DAK RIDGE NATIONAL LABORATORY
NUCLEAR DIVISION
X-10 LAB RECORDS DIVISION
P O BOX X
DAK RIDGE, TN 37830
OICV ATTN CIVIL DEF RES PROJ
OICV ATTN CENTRAL PSCH LIBRARY

SANDIA LABORATORIES
LIVERMORE LABORATORY
P O BOX 960
LIVERMORE, CA 94550
OICV ATTN LIBRARY & SECURITY CLASSIFICATION DIV.

SANDIA NATIONAL LAB
P O BOX 5800
ALBUQUERQUE, NM 87185
(ALL CLASS ATTN SEC CONTROL SEC FOR)
OICV ATTN A CHABAN
OICV ATTN I HILL
OICV ATTN DRC 1250 W BROWN
OICV ATTN A CHABIA
OICV ATTN W SCHERTY
OICV ATTN 3141
OICV ATTN L MORTMAN
OICV *Mr. J. Banister*

Remnant

OTHER GOVERNMENT

CENTRAL INTELLIGENCE AGENCY
WASHINGTON, DC 20505
OICV ATTN OSWR/NEC

DEPARTMENT OF THE INTERIOR
BUREAU OF MINES
Bldg 20, DENVER FEDERAL CENTER
DENVER, CO 80225
((UNCL ONLY))
OICV ATTN TECH LIP (UNCL ONLY)

DIRECTOR
FEDERAL EMERGENCY MANAGEMENT AGENCY
NATIONAL SEC OFC MITIGATION & RSCH
1725 I STREET, NW
WASHINGTON, DC 20472
((ALL CLASS ATTN B105 DCC CONTROL FCR))
OICV ATTN MITIGATION & RSCH DIV

DEPARTMENT OF DEFENSE CONTRACTORS

ACUREX CORP.
485 CLYDE AVENUE
MOUNTAIN VIEW, CA 94042
OICY ATTN C WOLF

AEROSPACE CORP.
P O BOX 92957
LOS ANGELES, CA 90009
OICY ATTN H HIRSH
OICY ATTN TECHNICAL INFORMATION SERVICES

AGRABIAN ASSOCIATES
257 N NASH STREET
EL SEGUNDO, CA 90245
OICY ATTN M AGRABIAN

ANALYTIC SERVICES, INC.
400 ARMY-NAVY DRIVE
ARLINGTON, VA 22202
OICY ATTN G HESSELBACHER

APPLIED RESEARCH ASSOCIATES, INC
2601 WYOMING BLVD NE SUITE E-1
ALBUQUERQUE, NM 87112
OICY ATTN J PRATT
OICY ATTN M HIGGINS

APPLIED THEORY, INC.
1010 WESTWOOD BLVD
LOS ANGELES, CA 90024
(2 CYS IF UNCLASS OR 1 CY IF CLASS)
OICY ATTN J TRULLIO

ARTEC ASSOCIATES, INC.
26046 EDEN LANDING ROAD
HAYWARD, CA 94545
OICV ATTN S GILL

ASTRON RESEARCH & ENGINEERING
1901 OLD MIDDLEFIELD WAY #15
MOUNTAIN VIEW, CA 94043
OICV ATTN J HUNTINGTON

AVCO RESEARCH & SYSTEMS GROUP
201 LOWELL STREET
WILMINGTON, MA 01837
OICV ATTN LIBRARY A630

BDM CORP.
7915 JONES BRANCH DRIVE
MCLEAN, VA 22102
OICV ATTN A LAVAGNINO
OICV ATTN T NEIGHBORS
OICV ATTN CORPORATE LIBRARY

BDM CORP.
P O BOX 9274
ALBUQUERQUE, NM 87119
OICV ATTN P HENSLEY

BOEING CO.
P O BOX 3707
SEATTLE, WA 98124
OICV ATTN S STRACK
OICV ATTN AEROSPACE LIBRARY
OICV ATTN M/S 42/37 R CARLSON

CALIFORNIA RESEARCH & TECHNOLOGY, INC.
6269 VARIEL AVENUE
WOODLAND HILLS, CA 91367
OICY ATTN LIBRARY
OICY ATTN K KREYENHAGEN
OICY ATTN M ROSENBLATT

CALIFORNIA RESEARCH & TECHNOLOGY, INC.
4040 FIRST STREET
LIVERMORE, CA 94550
OICY ATTN J ORZHAL

CALSPAN CORP.
P O BOX 400
BUFFALO, NY 14205
OICY ATTN LIBRARY

DENVER, UNIVERSITY OF
COLORADO SEMINARY
DENVER RESEARCH INSTITUTE
P O BOX 10127
DENVER, CO 80210
(ONLY 1 COPY OF GLASS PPTS)
OICY ATTN SEC OFFICER FOR J WISOTSKI

EG&G WASH. ANALYTICAL SVCS CO, INC.
P O BOX 10218
ALBUQUERQUE, NM 87114
OICY ATTN LIBRARY

ERIC H. WANG
CIVIL ENGINEERING DEPT FAC
UNIVERSITY OF NEW MEXICO
UNIVERSITY STATION
P O BOX 25
ALBUQUERQUE, NM 87131
OICY ATTN J LAMB
OICY ATTN P LORDE
OICY ATTN M BAHN
OICY ATTN J KOMARNA

GARD, INC.
7449 N NATCHEZ AVENUE
NILES, IL 60648
OICY ATTN G NEIGHARDT (UNCL ONLY)

GENERAL ELECTRIC CO.
SPACE DIVISION
VALLEY FORGE SPACE CENTER
P O BOX 8555
PHILADELPHIA, PA 19101
OICY ATTN M BORTNER

GENERAL RESEARCH CORP.
SANTA BARBARA DIVISION
P O BOX 6770
SANTA BARBARA, CA 92111
OICY ATTN JIC

HI-TECH LABS, INC.
P O BOX 1686
SANTA MONICA, CA 90406
OICY ATTN B HARTENBAUM

HORIZONS TECHNOLOGY, INC.
7830 CLAIREMONT MESA BLVD
SAN DIEGO, CA 92111
OICY ATTN R KRUGER

IIT RESEARCH INSTITUTE
10 W 25TH STREET
CHICAGO, IL 60616
OICY ATTN R FELCH
OICY ATTN M JOHNSON
OICY ATTN DOCUMENTS LIBRARY

INFORMATION SCIENCE, INC.
123 W PADRE STREET
SANTA BARBARA, CA 93105
OICV ATTN W DUDZIAK

INSTITUTE FOR DEFENSE ANALYSES
400 ARMY-NAVY DRIVE
ARLINGTON, VA 22202
OICV ATTN CLASSIFIED LIBRARY

J D HALTIWANGER CONSULT ENG SVCS
RM 106A CIVIL ENGINEERING BLDG
223 N DOMINE STREET
URBANA, IL 61801
OICV ATTN W HALL

J. H. WIGGINS CO., INC.
1650 S PACIFIC COAST HIGHWAY
REDONDO BEACH, CA 90277
OICV ATTN J COLLINS

KAMAN AVIONIC
82 SECOND AVENUE
NORTHWEST INDUSTRIAL PARK
BURLINGTON, MA 01203
OICV ATTN R RIETENIK
OICV ATTN LIBRARY
OICV ATTN M MORRIS
OICV ATTN F CRISCIONE

KAMAN SCIENCES CORP.
P O BOX 7463
COLORADO SPRINGS, CO 80933
OICV ATTN D SACHS
OICV ATTN F SHELTON
OICV ATTN LIBRARY

KAMAN TEMPO
816 STATE STREET (P O DRAWER 00)
SANTA BARBARA, CA 93102
OICV ATTN BASIAC

LOCKHEED MISSILES & SPACE CO., INC.
P O BOX 504
SUNNYVALE, CA 94086
OICV ATTN J WEISNER
OICV ATTN TIC-LIBRARY

MARTIN MARIETTA CORP.
P O BOX 5837
ORLANDO, FL 32855
OICV ATTN G ECTIEC

MARTIN MARIETTA CORP.
P O BOX 179
DENVER, CO 80201
OICV ATTN G FREYER

MCDONNELL DOUGLAS CORP.
5301 BOLSA AVENUE
HUNTINGTON BEACH, CA 92647
OICV ATTN H HERDMAN
OICV ATTN R HALPRIN
OICV ATTN D DEAN

MCDONNELL DOUGLAS CORP.
3855 LAKEWOOD BOULEVARD
LONG BEACH, CA 90846
OICV ATTN M POTTER

MERRITT CASES, INC.
P O BOX 1206
REDLANDS, CA 92373
OICY ATTN J MERRITT
OICY ATTN LIBRARY

METEOROLOGY RESEARCH, INC.
464 W WOODBURY ROAD
ALTADENA, CA 91001
OICY ATTN W GREEN

MISSION RESEARCH CORP.
P O DRAWER 719
SANTA BARBARA, CA 93102
(ALL CLASS: ATTN: SEC REC FOR)
OICY ATTN C LONGMIRE
OICY ATTN G MCCARTER

PACIFIC-SIERRA RESEARCH CORP.
1456 CLOVERFIELD BLVD
SANTA MONICA, CA 90404
OICY ATTN H BRODE

PACIFIC-SIERRA RESEARCH CORP.
WASHINGTON OPERATIONS
1401 WILSON BLVD
SUITE 1100
ARLINGTON, VA 22209
OICY ATTN D GORMLEY

PACIFICA TECHNOLOGY
P O BOX 149
DEL MAR, CA 92014
OICY ATTN R R JORK
OICY ATTN G KENT
OICY ATTN TECH LIBRARY

PATEL ENTERPRISES, INC.
P O BOX 2531
HUNTSVILLE, AL 35810
OICV ATTN M PATEL

PHYSICS INTERNATIONAL CO.
2700 MERCED STREET
SAN LEANDRO, CA 94577
OICV ATTN L DEHRMANN
OICV ATTN TECHNICAL LIBRARY
OICV ATTN F MOORE
OICV ATTN J THOMSEN
OICV ATTN E CAUER

P & D ASSOCIATES
P O BOX 9695
MARINA DEL REY, CA 90291
OICV ATTN R ROBT
OICV ATTN A KIRK
OICV ATTN J LEWIS
OICV ATTN W WRIGHT
OICV ATTN J CARPENTER
OICV ATTN TECHNICAL INFORMATION CENTER

RAND CORP.
1700 MAIN STREET
SANTA MONICA, CA 90406
OICV ATTN C MOY

SCIENCE APPLICATIONS, INC
RADIATION INSTRUMENTATION DIV
4615 HAWKINS, NW
ALBUQUERQUE, NM 87109
OICV ATTN J DUSON

SCIENCE APPLICATIONS, INC.
P O BOX 2351
LA JOLLA, CA 92039
OICV ATTN H HILSON
OICV ATTN TECHNICAL LIBRARY
OICV ATTN R SCHLAUG

SCIENCE APPLICATIONS, INC.
101 CONTINENTAL BLVD
EL SEGUNDO, CA 90245
OICY ATTN D HOWE

SCIENCE APPLICATIONS, INC.
2450 WASHINGTON AVENUE
SAN LEANDRO, CA 94577
OICY ATTN D BERNSTEIN
OICY ATTN D MAYWELL

SCIENCE APPLICATIONS, INC.
P O BOX 1303
MCLEAN, VA 22102
OICY ATTN J COCKAYNE
OICY ATTN B CHAMBERS III
OICY ATTN M KNASEL
OICY ATTN W LAYSON
OICY ATTN R SIEVERS

SOUTHWEST RESEARCH INSTITUTE
P O DRAWER 29510
SAN ANTONIO, TX 78284
OICY ATTN A MENZEL
OICY ATTN W BAKER

SRI INTERNATIONAL
333 PAVENSWOOD AVENUE
MENLO PARK, CA 94025
OICY ATTN G ABRAHAMSON
OICY ATTN LIBRARY
OICY ATTN J COLTON

SYSTEMS, SCIENCE & SOFTWARE, INC.
P O BOX 8243
ALBUQUERQUE NM 87108
OICY ATTN C NEEDHAM

SYSTEMS, SCIENCE & SOFTWARE, INC.
P O BOX 1620
LA JOLLA, CA 92038
OICY ATTN J PARTHEL
OICY ATTN T RINEY
OICY ATTN D CRINE
OICY ATTN LIBRARY
OICY ATTN C HASTING
OICY ATTN K PYATT
OICY ATTN C DISMUKES
OICY ATTN T CHERRY

SYSTEMS, SCIENCE & SOFTWARE, INC.
11900 SURPRISE VALLEY DRIVE
RESTON, VA 22091
OICY ATTN J MURPHY

TELEDYNE BROWN ENGINEERING
GIMMINGS RESEARCH PARK
HUNTSVILLE, AL 35897
OICY ATTN J RAVENSCRAFT
OICY ATTN J MCSHAFF

TERRA TEK, INC.
420 WAKAPA WAY
SALT LAKE CITY, UT 84108
OICY ATTN A ABOU-SAYED
OICY ATTN LIBRARY
OICY ATTN A JONES
OICY ATTN S GREEN

TETRA TECH, INC.
437 N ROSEMEAD BLVD
PASADENA, CA 91107
OICY ATTN L HWANG

TRW DEFENSE & SPACE SYS GROUP
ONE SPACE PARK
REDONDO BEACH, CA 90278
OICY ATTN N LIPNER
OICY ATTN TECHNICAL INFORMATION CENTER
OICY ATTN T MAZZOLA

TRW DEFENSE & SPACE SYS GROUP
P O BOX 1310
SAN BERNARDINO, CA 92407
OICY ATTN G HILCHER
OICY ATTN P DAI
OICY ATTN F WONG

UNIVERSAL ANALYTICS, INC.
7740 W MANCHESTER BLVE
PLAYA DEL REY, CA 90291
OICY ATTN F FIELD

WEIDLINGER ASSOC., CONSULTING ENGINEERS
117 E 59TH STREET
NEW YORK, NY 10022
OICY ATTN I SANDLER
OICY ATTN M PADER

WEIDLINGER ASSOC., CONSULTING ENGINEERS
3000 SAND HILL ROAD
VENUE PARK, CA 94026
OICY ATTN J ISENBERG

*Chief Scientist
Naval Research Laboratory
Laboratory for Computational Physics
Code 4040
Washington, D.C. 20375
100CY Attn J. Boris*